Stability Determination of the Modified Activated Carbon to Adsorb Thiophenic Compounds from Model Diesel Fuel

Moradi, Sajad
Chemical Engineering Faculty, Tarbiat Modares University, P.O. Box 14155-4838 Tehran, I.R. IRAN

Moosavi, Elham
Department of Chemical and Materials Engineering, Buein Zahra Technical University, Buein Zahra, Qazvin, I.R. IRAN

Karimzadeh, Ramin*+
Chemical Engineering Faculty, Tarbiat Modares University, P.O. Box 14155-4838 Tehran, I.R. IRAN

ABSTRACT: *The main objective of this research is stability determination of activated carbon adsorbent at fixed bed adsorption column for desulfurization of diesel fuel by mathematical modeling. This model is based on mass balances. Equations that are the outcome of mass balances are known as the second degree of partial differential equations, and they must be solved together simultaneously to generate appropriate breakthrough curves at the end of the bed. On the other hand, running momentum balance by using some assumptions, lead to the Ergun equation which clearly represents pressure drop through adsorption bed. The mentioned equations have been solved simultaneously in MATLAB software and the solution method was the finite difference. After ensuring the validity of the model, scaling up is done to determine adsorbent stability and quantify its performance in an industrial dimension bed. Then the effective parameters on the bed operation and adsorbent stability were identified. Also, the batch adsorption isotherm experiments were carried out at room temperature to determine the maximum capacity of adsorbent in sulfur compound adsorption. Using capped bottles containing 10 mL solutions which contain dibenzothiphen (DBT) dissolved in n-decane and 0.1 g of activated carbon that were equilibrated for 5 hours. Concentrations of* Thiophenic Compound *(TC) solutions were 330,462,660,990, and 1,320 mg/L of TC. The experiment method was according to some author's studies. The fluid velocity and mass transfer resistance for diffusion in adsorbent's pores are the most important parameters in adsorption bed's behavior and generating of breakthrough curves. The lowest the fluid velocity, the more time the fluid stays in bed and the bed's efficiency raises in terms of pollutant removal accordingly, as well as bed saturated in a longer time.*

KEYWORDS *Adsorption, Mathematical Modeling, Desulfurization, Diesel Fuel, Activated Carbon, Stability.*

** To whom correspondence should be addressed.*
+ E-mail: ramin@modares.ac.ir
1021-9986/2019/4/149-165 17/$/6.07

INTRODUCTION

Production of clean hydrocarbon fuels, i.e. with low sulfur and aromatic content, has become one of the most important tasks of a modern petroleum refinery [1, 2]. Sulfur in diesel and gasoline contributes to environmental pollution via the formation of sulfur dioxide (SO_2) during fuel combustion. SO_2 is responsible for acid rain, which has detrimental effects on the ecosystem, structures and human health. In addition, sulfur present in fuel causes poisoning of the catalysts in catalytic converters of vehicles [3, 4].

The new regulations brought down the sulfur level of diesel from about 400 to 500ppm (parts per million on a weight, basis) to 15 ppm. Ultra Low Sulfur Diesel (ULSD) fuel of less than 50ppm became the specification in both the European Union and Japan in 2005. The European commission further adopted a 10ppm sulfur specification for road diesel fuel beginning January 1st, 2005 with full conversion by 2010. An U.S. EPA rule of 15ppm sulfur highway diesel fuel was implemented on June 1st, 2006 [5]. U.S. pipelines are anticipated to include a plan to deliver a sulfur level below 10ppm fuel. In 2007, Japan proposed a sulfur level of 10 ppm in their fuel. Several countries in other regions of the world are also working to reduce the sulfur content in diesel fuel. Conventional hydrodesulfurization (HDS) processes have been employed extensively by refineries to remove organic sulfur compounds from fuels for several decades and the lowest sulfur content achieved by such processes is around 500 ppm, although ULSD can be achieved by using deep HDS. However, to meet the challenges of producing ultra-clean fuels with sulfur content lower than 15 ppm, both capital investment and operational costs would increase due to more severe operating conditions [5, 6]. It is generally known that most of the sulfur compounds in deeply desulfurized (i.e. S < 10 ppmw) fuels *via* the HDS method are attributed to refractory species, namely alkylated dibenzothiophenes (DBTs). Typical examples include (but are naturally not limited to) 4,6-dimethyl- DBT, 4,6-diethyl-DBT and also C3- and C4-DBTs [7, 8].

Use of adsorption processes in the chemical industry are some of the most economically attractive methods for the separation of a pollutant from a gaseous or a fluid stream and it is because of the straightforward operating conditions and availability of inexpensive and re-generable adsorbents including zeolites, metal-based adsorbents, silica, alumina, and activated carbon [3, 9,12-14].

Activated carbons and zeolites have been widely used as adsorbents in the separation and purification processes for gaseous or aqueous solution systems [1, 15]. *Faghihian et al.* studied on desulfurization of gas oil by modified clinoptilolite. Clinoptilolite is a naturally occurring zeolite, formed by the diversification of volcanic ash in the lake and marine waters millions of years ago. It is an abundant natural zeolite. They show that Hg+2 and Ag+ clinoptilolite can adsorb sulfur compounds from commercial fuels selectively and with high capacities [16]. Also, *Bazmi et al.* worked on sulfur compounds adsorption onto nano AgX-zeolites and their regeneration. The influence of variables in the process consists of adsorbent metal percent (0.05-10 wt%), adsorbent calcination temperature (200-500 °C) and adsorption process temperature (30-120 °C) in adsorption stage and gas flow rate (1.5-3.5 mL/Min), regeneration temperature (150-300 °C) and desorption time (30-90 Min) which were investigated using experimental design procedure. The contours show that the increasing metal percentage decreases sulfur compounds adsorption and by increasing calcination temperature sulfur compounds adsorption increases. Also by increasing the gas flow rate, desorption time and desorption temperature increase regeneration efficiency [17].

Activated carbons due to their low cost, high specific surface area, thermal and chemical stability under anoxic conditions, receptivity for modification, and high affinity toward adsorption of aromatic and refractory sulfur compounds have been extensively studied for the removal of TC from different fuels [9, 18].

Also, some other adsorbents were used in the desulfurization process. For example, *Kazemzad et al.* studied the application of spherical mesoporous silica MCM-41 for adsorption of dibenzothiphene from model oil. Their results showed that 0.03 g/mL of mesoporous silica has the capability to adsorb more than 42% of DBT (sulfur containing compound) from the dodecane solution. The improvement of mass transfer via adsorption DBT by the prepared nanosorbent is an efficient method for enhancement of biodesulfurization kinetic [19].

Based on the operation mode, adsorption can be generally classified into static adsorption and dynamic adsorption. Static adsorption also called batch

adsorption occurs in a closed system containing a desired amount of adsorbent contacting with a certain volume of adsorbate solution, while dynamic adsorption usually occurs in an open system where adsorbate solution continuously passes through a column packed with the adsorbent. For column adsorption, the way to determine the breakthrough curve is a very important issue because it provides the basic but predominant information for the design of a column adsorption system. Without the information of the breakthrough curve, one cannot determine a rational scale of column adsorption for practical application. There are two widely used approaches to obtain the breakthrough curve of a given adsorption system: direct experimentation or mathematical modeling. The experimental method could provide a direct and concise breakthrough curve of a given system. However, it is usually a time-consuming and economical undesirable process, particularly for the trace contaminants and long residence time. Also, it greatly depends upon the experimental conditions, such as ambient temperature and residence time. Comparatively, mathematical modeling is simple and readily realized with no experimental apparatus required, and thus, it has attracted increasing interest in the past decades [20].

Due to the amount of solute adsorbed and adsorbent required and also the important impact of operating time on the effective use of the column, at an industrial scale, the end time operation, that the bed has become saturated, must be determined after an environmental and economic evaluation and of the process. One way to optimize the operating conditions and other mentioned parameters can be performed by means of mathematical modeling [14, 21]. Mathematical models can be useful in designing where; we need to decide about bed specifications such as the cross sectional area and length and of the bed, the size of adsorbent particles and the amount of them, the bed porosity and the other operation conditions [22].

On the other hand, mathematical modeling is simple and does not require any experimental apparatus. Besides, mathematical models facilitate the design and analysis of large scale processes by decreasing the number of pilot scale tests to evaluate several operating parameters. Currently, a variety of mathematical models have been used to describe and predict the breakthrough curves of a column adsorption system in liquid or gaseous phase [20, 23, 24].

Fatemi et al. in the experimental study and adsorption modeling of COD reduction by activated carbon for wastewater treatment of oil refinery, by assuming that the system operates under isothermal conditions and the pressure drop throughout the column is negligible, by applying mass balance in the fluid phase, dynamic modeling of adsorption bed was performed and the resulting differential equations were solved numerically by a Method of Line technique. The numerical algorithm is developed and implemented into a computer program using MATLAB (R.2007b) software. Mass transfer and the other key parameters were obtained and finally by adjusting and modifying the pollutant mass transfer parameters, they proposed some suggestions for scale up of the dynamic adsorption process [10].

Shams and *Dehkordi* work on Desulfurization of Liquid-Phase Butane by Zeolite Molecular Sieve 13X in a Fixed Bed, by modeling, simulation, and comparison with commercial-scale plant data. The model equations account for the effect of axial dispersion and the inter- and intraparticle mass-transfer resistances at isothermal operating conditions. Orthogonal collocation and Gill's fourth-order Runge–Kutta methods were used to solve the dimensionless general forms of the 4N-coupled ordinary differential equations for simultaneous adsorption of the solutes by the adsorbent in a fixed bed. The model predictions were compared to the commercial-scale plant data of an Iranian petrochemical company (Bandar Imam, Iran). Moreover, the influences of the bed Reynolds number, Peclet number, total inlet sulfur concentration, feed temperature, and diameter of the spherical adsorbent on the breakthrough curve were investigated [13].

Yusuff et al. in Mathematical Modeling of Fixed Bed Adsorption Column for Liquid Phase Solute developed a mathematical model for pseudo one component adsorption on a fixed bed. The model takes into account external and internal mass transfer resistances with non-ideal plug flow behavior. In the present study, the Langmuir equilibrium isotherm is used to represent the liquid-solid equilibrium relationship. The model consists of a set of couple partial differential equations, and the differential equations representing the mass balances of both fluid and pore phases are solved by the implicit backward Euler finite difference method and compared with previous models reported in the literature. The effects of various important and influencing parameters such as

flow rate, particle radius and bed porosity in the breakthrough curve are studied in detail [11].

Since in an industrial unit, the adsorbent operation time, hence the time that it can efficiently adsorb pollutant, is important, the main goal of this paper is to introduce the dynamic modeling of a fixed bed based on mass balance for adsorptive desulfurization process and scale up to a large industrial unit to stability determination of adsorbent. Also, the effect of different operating parameters on stability has been investigated, and then the effective parameters on the bed operation and adsorbent stability were identified.

MATHEMATICAL MODELING

In adsorption, when the fluid phase and solid phase are contacted with each other, mass transfer of fluid phase towards the adsorbent takes place. The molecules of the fluid phase which diffuse into the adsorbent surface, faced with resistances that reduce the rate of their diffusion and the mass transfer. In this process, there are two main steps, film mass transfer (external) and intraparticle diffusion (internal) as shown in Fig. 1.

According to some authors [20, 25] to model a liquid-solid column adsorption, it is necessary to divide into the four basic steps:

1- Liquid phase mass transfer including convective mass transfer and molecular diffusion.

2- Interface diffusion between the liquid phase and the external surface of adsorbent (film diffusion).

3- Intrapellet mass transfer involving pore diffusion or surface diffusion or both of them the adsorption reaction

4- The adsorption- desorption reaction

Although in various models the assumptions and conditions can vary, mostly there are three main steps in all of them which have been applied in developing the models [22]:

1- The mass, heat and momentum balances for bulk fluid in the bed.

2- The mass and heat balances within the particles.

2- The adsorption isotherm correlations.

The mass, energy and momentum balance equations in both fluid and solid phase are based on the following assumptions:

1- The temperature gradient due to the low heat of adsorption is negligible.

2- The process is isothermal and the bed keeps at a uniform temperature.

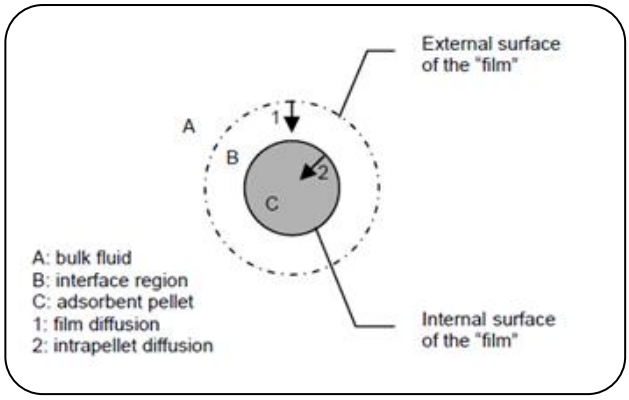

Fig. 1: Mass conservation in a control volume [20].

3- Pressure drop in the axial direction of the bed is considered.

4- Considering the fluid velocity is low, axial dispersion in the bed should be account and its coefficient will be calculated with the correlative equation.

5- The adsorbent pellets have uniform size and are identical and uniformly distributed in the bed.

6- The bed is divided into K equal sections. The length of each section is dz:

dz= L/K

7- The radial distribution of solute in the bed is neglected.

8- There no change in porosities of the particles and bed.

9- The feed flow rate is constant so there is no variation in fluid velocity in the bed.

10- The density and viscosity of the fluid during the adsorption are constant.

11- The mass transfer rate is represented by the linear driving force model between the saturated and loaded solid concentrations.

12- There is no chemical reaction occurs.

Mass Transfer in the Bed

Concerning a control volume as shown in Fig. 2, we can set a mass balance as follow:

$$\varepsilon_b D_{az} \frac{\partial^2 C}{\partial z} - (1-\varepsilon_b)\frac{\partial q}{\partial t} = \varepsilon_b \frac{\partial C}{\partial t} \quad (1)$$

Mass transfer into the adsorbent particles that is written as $\rho_s \frac{\partial q}{\partial t}$ can be replaced by a linear rate of the fluid film as follow:

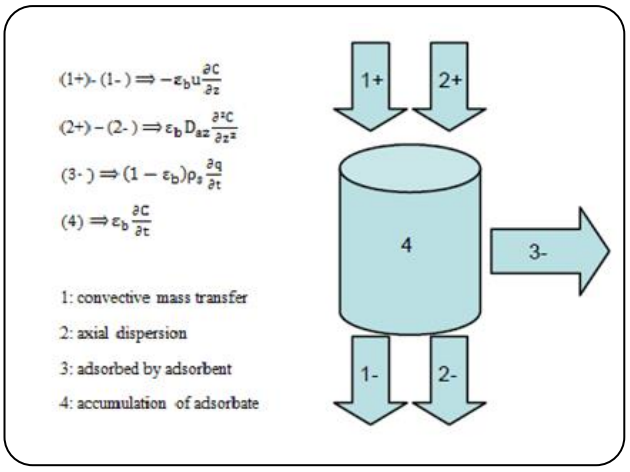

Fig. 2: Mass conservation in a control volume [20].

$$\left(1-\varepsilon_b\right)\frac{4}{3}\pi R_p^3\rho_s\frac{\partial q}{\partial t}=\left(1-\varepsilon_b\right)4\pi R_p^2 k_m\left(C-C_p\big|_{r=R_p}\right) \quad (2)$$

Then we have:

$$\varepsilon_b D_{az}\frac{\partial^2 C_i}{\partial z^2}-\varepsilon_b u\frac{\partial C_i}{\partial z}-\frac{3\left(1-\varepsilon_b\right)}{R_p}k_m\left(C_i-C_p\big|_{r=R_p}\right)= \quad (3)$$

$$\varepsilon_b\frac{\partial C_i}{\partial t}$$

Where the initial and boundary conditions of this equation are:

$$t=0\ \cdot\ z=0:\ C_i=C_{io} \quad (4)$$

$$t=0\ \cdot\ 0<z\le L:\ C_i=0 \quad (5)$$

$$t>0\ \cdot\ z=0:\ \varepsilon_b D_{az}\frac{\partial C_i}{\partial z}u\left(C_{io}-C_i\right) \quad (6)$$

$$t>0\ \cdot\ z=L:\ \frac{\partial C_i}{\partial z}\bigg|_{z=L}=0 \quad (7)$$

The intra-pellet mass transfer is due to the diffusion of adsorbate molecules through the pore is written as:

$$\varepsilon_b\frac{D_{pi}}{r^2}\frac{\partial}{\partial r}\left(r^3\frac{\partial C_{pi}}{\partial r}\right)=\left[\varepsilon_b\frac{\partial C_{pi}}{\partial t}+\left(1-\varepsilon_p\right)\rho_s\frac{\partial q_i}{\partial t}\right] \quad (8)$$

With initial and boundary conditions as follow:

$$t=0:\ C_p=0\ .\ q_i=0 \quad (9)$$

$$r=0\ :\ \frac{\partial C_{pi}}{\partial r}=0 \quad (10)$$

$$r=R_p\Rightarrow\varepsilon_b D_p\frac{\partial C_{pi}}{\partial r}\bigg|_{r=R_p}=k_m\left(C_i-C_{pi}\big|_{r=R_p}\right) \quad (11)$$

By using the Langmuir isotherm adsorption equation:

$$q=\frac{q_m K C_p}{1+K C_p} \quad (12)$$

$$D_p\varepsilon_b\left[\frac{1}{r^2}\frac{\partial}{\partial r}\left(r^2\frac{\partial C_p}{\partial r}\right)\right]= \quad (13)$$

$$\left(\varepsilon_p+\rho_s\left(1-\varepsilon_p\right)\frac{q_m K}{\left(1+K C_p\right)^2}\right)\frac{\partial C_p}{\partial t}$$

The Equations (3), (8) and (13) were in agreement with numerous authors' studies [13, 20, 22, 29, 30].

Diffusion coefficient in dilute solutions of fluid can be calculated from the Wilke-Chang equation [26, 27]:

$$D_m=7.4\times10^{-8}\frac{\left(\varphi_B M_B\right)^{0.5}T}{\mu\vartheta_A^{0.6}} \quad (14)$$

The effective diffusion coefficient into the adsorbent is lower than the diffusion coefficient into a direct cylindrical pore. One of the relationships that correspond these two factors together is [28]:

$$D_p=\frac{1}{\tau_p}D_m \quad (15)$$

Tortuosity is one of the key parameters describing the geometry and transport properties of a porous solid. Estimating the Tortuosity factor is possible by giving pore structure, pore size and shape distribution, however, some approximate relations in various references are provided to predict this factor [28]:

$$\tau_p=\frac{1}{\varepsilon_p} \quad (16)$$

$$\tau_p=\frac{\left(1-\varepsilon_p\right)^2}{\varepsilon_p} \quad (17)$$

$$\tau_p=\varepsilon_p+1.5\left(1-\varepsilon_p\right) \quad (18)$$

The axial dispersion coefficient is calculated through the following equation [28]:

$$\frac{D_{az}}{D_{mi}} = \gamma_1 + \gamma_2 \frac{d_p u}{D_{mi}} = \gamma_1 + \gamma_2 \frac{(Re)(Sc)}{\varepsilon_b} \quad (19)$$

Where Reynolds number, Schmidt number, γ_1 and γ_2 are defined as:

$$Re = \frac{\varepsilon_b u d_p}{\vartheta} \quad (20)$$

$$Sc = \frac{\vartheta}{D_{mi}} \quad (21)$$

$$\gamma_1 = 0.45 + 0.55\varepsilon_b \quad (22)$$

$$\gamma_2 = 0.5\left(1 + \frac{13\gamma_1\varepsilon}{ReSc}\right)^{-1} \quad (23)$$

According to Ruthven, to prevent attrition from the movement of particles within the bed it is normal practice to limit the allowable velocity in up flow to less than about 80% of the minimum fluidization velocity [29]:

$$u_{max} = 6\times10^{-4} g \frac{(2Rp)^2}{\mu}(\rho_s - \rho_f) \quad (24)$$

The overall mass transfer is caused by two mass transfers that the first is mass transfer resistance in fluid film and the second is resistance in adsorbent pores. The overall resistance is governed by:

$$\frac{1}{k_m} = \frac{1}{k_f} + \frac{1}{k_s} \quad (25)$$

The film mass transfer coefficient, k_f, can be obtained from Sherwood number correlation [28]:

$$k_f = \frac{ShD_{mi}}{d_p} \quad (26)$$

The mass transfer coefficient of fluid in adsorbent pores is calculated through the following equation [29]:

$$k_s = \frac{5\varepsilon_p D_p}{d_p} \quad (27)$$

At the same time solving fluid, pellet and equilibrium equations with initial and boundary condition for fluid and pellet equations, $C_{p,q}$ and C obtained at different time and place but solving such a large differential equation is possible only by means of numerical methods by using a computer program.

Pressure Drop through the Bed

Clearly, the resistance to fluid flow through the porous medium is related to the number of particles present. The resistance to the fluid flow gives rise to a pressure drop in the fluid. The pressure decreases in the direction of fluid velocity. The pressure drop equation is defined by the Ergun's equation which can cover all the flow regimes as [26]:

$$\frac{\Delta P}{L} = \frac{150u\mu}{g_c\varphi_3^2 D_p^2}\frac{(1-\varepsilon)}{\varepsilon^3} + \frac{1.75u^2\rho}{g_c\varphi_3 D_p}\frac{1-\varepsilon}{\varepsilon^3} \quad (28)$$

Numerical solution of the nonlinear preceding sets of partial differential equations derived from mass balances was conducted by a reduction to set of ordinary differential equations with respect to the time derivative terms using an implicit finite difference method. A mathematical algorithm to solve these coupled equations was developed and implemented into a computer program using MATLAB software.

The performance of packed beds is described through the concept of a breakthrough curve. A breakthrough curve is a plot of the concentration at a fixed point in the bed, usually at or near the outlet, versus time. Alternatively, it can be plotted in the dimensionless form by dividing the effluent concentration by the inlet concentration, *Ce/Cin*, so that the vertical coordinate varies between zero and one, at which point the bed is saturated. The breakthrough point is the point in the diagram at which the outlet concentration reaches a value predetermined as the air purifying objective. Thus the adsorbent needs to be replaced. This point varies depending on the type of contaminant [22].

EXPERIMENTAL SECTION

In the experimental section, equilibrium sorption experiments were conducted to find proper adsorption isotherms and maximum adsorption capacity of adsorbent from model diesel solution which contains DBT as a refractory compound. The information that achieved in this section is very important in modeling and particular dimension design.

Adsorption Isotherms

Adsorption isotherm experiments of dibenzothiphen on activated carbon adsorbent were carried out at room temperature using capped bottles containing 10 mL single-solute solutions and 0.1 g of activated carbon that were equilibrated for 5 h. This amount of solution and adsorbent and the ratio is in agreement with another study done by Moosavi et.al [9]. Each solution contained only DBT dissolved in *n*-decane. Initial concentrations of thiophenic solutions were 300, 500, 600, 990, 1200, 1400 and 1500 mg DBT/L solvent. Equilibrium time was set 5 h according to [31, 32]. Concentrations of DBT in filtered equilibrated solutions were determined by UV spectroscopy method. TC uptake was calculated from the equation:

$$q_e = \frac{V\left(C_o - C_e\right)}{m} \tag{29}$$

Where qe is the adsorbed amount (mg sulfur/g adsorbent), V is the volume of solution (L), C0 and Ce are initial and equilibrium concentrations (mg sulfur/L), and m is the mass of adsorbent (g).

Material Preparation

A commercial activated carbon was used as an adsorbent in this study. n-decane (99.9% purity) was obtained from Dr. Mojalali Company (Tehran, Iran) and the dibenzothiphen sample (>99% purity) was purchased from Merck (Hohenbrunn, Germany).

Specific surface area and pore size distribution of carbon products were determined from adsorption isotherms of nitrogen from relative pressure (P/P0) of 10−6 to 1 at 77K using a Micrometrics ASAP instrument. Samples were degassed in vacuum for 5 h at 180 °C prior to nitrogen adsorption. Specific surface area (SBET) was calculated from the linear range of the Brauner-Emmett-Teller (BET) equation in the relative pressure of 0.01 to 0.1. Microspore volume ($V_{micro,\ DR}$) was calculated from the Dubinin-Radushkevich (DR) equation in the relative pressure range of 10−5 to 10−1. Total meso- and macrospore volume ($V_{meso+macro}$) was calculated by subtracting the estimated microspore volume from the total volume. Pore size (volume) distribution was determined from nitrogen isotherms employing the Micrometrics' Density Functional Theory (DFT) software using a graphite model with slit shape geometry and considering a low degree of regularization or data smoothing (λ= 0.005). Total pore volume (V_{total}) was calculated from the adsorbed volume of nitrogen near the saturation point (P/P0 = 0.98). Concentrations of DBT in *n*-decane were determined using a UV spectrophotometer instrument (Optizen 3220 UV) at 325 nm wavelengths according to *Moosavi* [9].

RESULTS AND DISCUSSION

To investigate the experimental data validity with adsorption isotherms relations, we use the linear form of Langmuir and Freundlich isotherms as follow and the results are shown in Fig. 3 and Table 1:

$$\frac{1}{q} = \frac{1}{q_m K_L}\frac{1}{C_e} + \frac{1}{q_m} \tag{30}$$

$$Lnq = LnK_F + \frac{1}{n}LnC_e \tag{31}$$

The results of the matching of experimental data with adsorption isotherms indicate that both Langmuir and Freundlich isotherms well predict the behavior of the adsorption process.

Since in scale up and in the absorption bed calculation, to obtain the amount of adsorbent required we need the equilibrium capacity of adsorbent, and since this is one of the parameters of the Langmuir isotherm equation so Langmuir isotherm is chosen and gives us the possibility to directly reach this number.

Validity of Model

To validate the model, we use experimental data of *Muzic et al.* [1], whose study focused on the desulfurization of diesel fuel in dynamic fixed bed adsorption. Adsorbent properties and their bed's dimensions are given in their paper. Also, a commercial diesel produced one of the refineries in Croatia used as fuel in their study and the initial concentration of sulfur in fuel was 27 ppm.

Experiments done in the dynamic adsorption system consist of a cylindrical bed. A feed with various flow rates entered into the bed and outlet concentration breakthrough curves versus time were obtained. The effect of feed velocity and bed length were investigated. Also, the final outlet concentration was set at 10 ppm and meets this point the operation should be stopped and the bed is regenerated. Comparisons between presented models

Table 1: Results of adsorption equilibrium analysis.

Langmuir isotherm constants					Freundlich isotherm constants		
q_m (mg S/g)	q_m (mg DBT/g)	K_L (kg/mg S)	K_L (kg/mg DBT)	R^2	K_F (mg-DBT/g Ads)* (kg-Sol/mg-DBT)$^{1/n}$	n	R^2
24.5	140.85	0.122	0.021	0.9528	5.59	1.59	0.9817

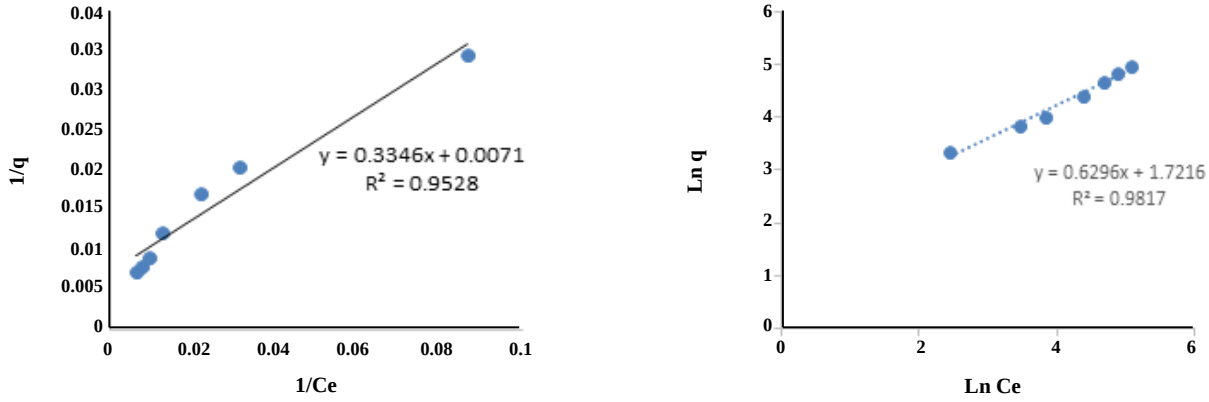

Fig. 3: Adsorption isotherm of DBT on the activated carbon. Solid lines represent linear form of isotherm equation fit of the data. (a) Langmuir isotherm (b) Freundlich isotherm

with experimental data obtained in Muzic work are shown in Fig. 4. Experimental data are obtained in a bed with a diameter of 2.2 cm and a length of 28.4 cm and a feed flow rate of 5 cm^3/ min. As mentioned above, allowable concentration in output was set 10 ppm and after reaching this point, the feed should into the new bed. Time to reach this concentration has been reported in laboratory 13.5 minutes, while the time of 13.7 minutes with our proposed model is obtained.

In addition to validating the model presented in Fig. 4, according to *Legates et al.* [33], one of the most perfect ways to evaluate the model, is measuring a combined relative error (R^2) and absolute error (RMSE) respectively:

$$RMSE = \sqrt{MSE} \tag{32}$$

$$MSE = \frac{SSE}{n} \tag{33}$$

$$SSE = \sum_{i=1}^{n} \left(C_{exp,i} - C_{mod,i} \right)^2 \tag{34}$$

$$R^2 = 1 - \frac{SSE}{SST} \tag{35}$$

$$SST = \sum_{i=1}^{n} \left(C_{exp,i} - \bar{C}_{exp} \right)^2 \tag{36}$$

We used the experimental data reported in *Muzic et al.* [1] to validate the model presented in this paper. The results have been presented in Table 2. The relative error has been made 0.95.

According to given combined relative error (R^2) obtained from the above expressions, in confirming the result obtained in Fig. 4, we can conclude that the proposed mathematical model is suitable for predicting the behavior of a dynamic absorption fixed bed. So the scale up calculation can be done based on the results obtained from this model.

Scale Up

Considering an industrial unit with 1 ton/h with 5000 ppm to 10000 ppm sulfur, we are going to reduce this sulfur level to 500 ppm by means of fixed bed adsorption. For this purpose, we follow two methods. First, considering the feed velocity on a large scale the same as the experimental scale in Muzic work, since the flow rate makes change, we obtain the large bed's diameter.

Table 2: The model deviation from experimental data.

SSE	MSE	RMSE	SST	R^2
22.812	1.406	1.068	459.885	0.95

Table 3: Required parameters for simulation

Parameters	Unit
Bed Diameter	cm
Bed Length	cm
Adsorbent pellet diameter	cm
Initial concentration of sulfur	ppm
Temperature	K
Pressure	bar
Feed volumetric flow rate	m^3/h
Bed porosity	-
Adsorbent porosity	-
Adsorbent bulk density	kg/m^3
Feed density	kg/m^3
Feed viscosity	cP

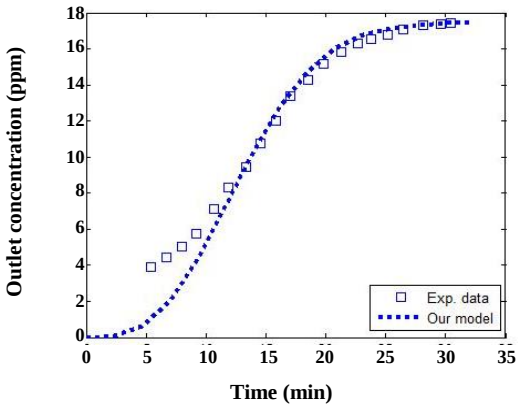

Fig. 4: Model validation with Muzic experimental data.

In a second way, by using the maximum allowable velocity of feed in the bed, we calculate the diameter. Also, we can select a velocity between the two values mentioned above as a middle velocity and repeat the calculation. The parameters required as an input to the software are listed in Table 3.

According to Mc. Cabe [26], in designing a fixed bed adsorption column, some parameters should be considered as follow:

- Select the type of adsorbent and its size.
- Select the appropriate fluid velocity to obtain a cross section of the bed.
- Obtain the bed length for given cycle time or calculate the breakthrough time for a selected bed length.

Calculating the Bed Diameter by Using Mc. Cabe Method

According to Mc. Cabe [26], in scale up, superficial velocity and adsorbent pellets diameter are the same on both large scale and small scale. The bed height and required amount of adsorbent are obtained given bed volume and desulfurization level. In the small scale with a volumetric flow rate of 5 cm^3/min and given bed diameter of 2.2 cm, the superficial velocity will be 1.314 cm/min. We use this value as a superficial velocity on a large scale. With a flow rate of large scale and superficial velocity, it is possible to calculate the bed cross section area and consequently the bed diameter.

$$Q = 20202\,cm^3/min$$

$$A = \frac{Q}{u} = 1.530\,m^2 \Rightarrow D = \sqrt{\frac{4A}{\pi}} = 1.4m$$

It is better to consider 1.5 m instead of 1.4 m. Therefore, the cross area value changes to 1.767 m^2.

If the initial concentration of sulfur was 10000 ppm and reducing this value to 500 ppm was our goal, so the amount of sulfur in the inlet is:

$$10000\text{ppmS}=10\frac{\text{kgS}}{\text{h}}$$

And the amount of sulfur in the outlet is:

$$500\text{ppmS}=0.5\text{kgS}$$

So, 9.5 kg S should be adsorbed. Using Langmuir equilibrium adsorption isotherm data, it was found that the adsorbent is able to adsorb 24.5 g sulfur/ g Ads. :

$$9.5\frac{\text{kgS}}{\text{h}}=388\frac{\text{kgAds}}{\text{h}}$$

By given the bulk density of adsorbent, $480\frac{\text{kgAds}}{\text{m}^3\text{Ads}}$, the volume of the bed can be obtained:

$$388\frac{\text{kgAds}}{\text{h}}=0.808\frac{\text{m}^3\text{Ads}}{\text{h}}$$

Now, by using the volume and cross area, the bed length is:

$$\text{L}=\frac{0.808}{1.767}=0.46\text{m}$$

A bed with a diameter of 150 cm for reducing the sulfur concentration from 10000 ppm to 500 ppm, requires at least 46 cm as length, but since a bed with this dimensions, that so-called fat bed, is not conventional, for various reasons, for example, channeling in the bed etc., we select integer ratio of diameter for bed height and the bed saturation time (i.e. reach to 500 ppm) is obtained by means of software. The result has been shown in Fig. 5 and Table 4.

Calculating the Bed Diameter by Using Maximum Allowable Fluid Velocity

Ruthven et al. [29] provided a relation for maximum fluid velocity in packed bed as follow:

$$u_{max}=6\times10^{-4}g\frac{(2Rp)^2}{\mu}\left(\rho_s-\rho_f\right) \quad (24)$$

$$u_{max}=12\frac{\text{cm}}{\text{min}}$$

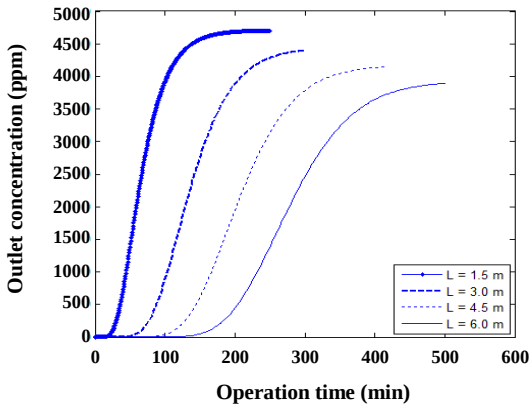

Fig. 5: Fixed bed performance at different length for the lowest velocity (u= 1.314 cm/ min).

The bed diameter and length are obtained by a method that mentioned before, and also the saturation time is obtained by means of software. The results are shown in Fig. 6 and reported in Table 5:

$$\text{D}=46\text{ cm}\Rightarrow\text{D}=0.5\text{ m}$$
$$\text{L}=0.410\text{ m}$$

As shown in Fig. 6 it can be used two parallel beds with a height of 4.1 m and feed flow rate of 500 kg/h instead of a bed with 8.2 m and 1000 kg /h respectively.

Calculating the Bed Diameter by another Method

The fluid velocity in the first method and second methods were 0.0219 cm/s and 0.2 cm/s respectively. These values lead to beds with diameters of 1.5 m and 0.5 m respectively. By select the bed diameter to 1 m which is between the two values obtained before, the new velocity is between 0.0219 to 0.2 cm/s:

$$\text{D}=100\text{ cm}\Rightarrow\text{u}=2.574\frac{\text{cm}}{\text{min}}$$

The new length of the bed is calculated:

$$\text{L}=1.03\text{ m}$$

Here, to avoid design a fat bed, we select integer ratio of diameter for bed height and the bed saturation time (i.e. reach to 500 ppm) is obtained by means of software. The result has been shown in Fig. 7 and Table 6.

The results of the three different methods to scale up to have been shown in Fig. 8. It is obvious that the effect of fluid velocity in the bed is significant. Whatever the fluid

Table 4: Comparison of fixed bed operation at different lengths for the lowest velocity (u= 1.314 cm/min).

Variable	Bed diameter	Bed length	Saturation time
Unit	cm	cm	min
Value	150	150	36
	150	300	88
	150	450	145
	150	600	204

Table 5: Comparison of fixed bed operation at different lengths for a maximum allowable velocity (u= 12 cm/min).

Variable	Bed diameter	Bed length	Saturation time
Unit	cm	cm	min
Value	50	410	14
	50	820	30
	50	2*410	28

Table 6: Comparison of fixed bed operation at different lengths for a selected velocity (u= 2.574 cm/min).

Variable	Bed diameter	Bed length	Saturation time
Unit	Cm	cm	min
Value	100	200	23
	100	300	39
	100	400	55
	100	500	72

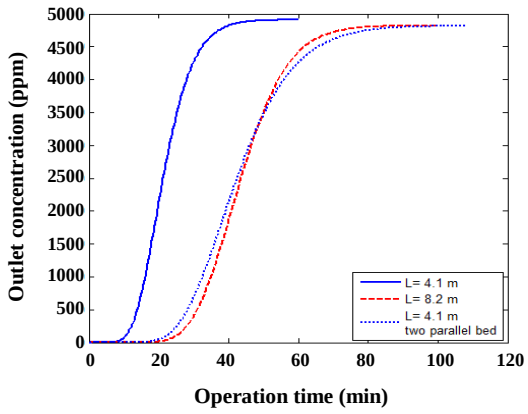

Fig. 6: Fixed bed performance at different length for a maximum velocity (u= 12 cm/ min).

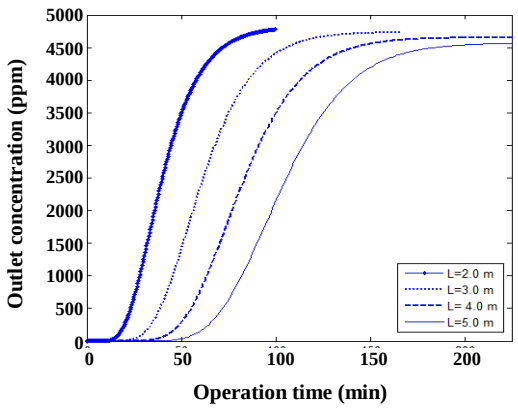

Fig. 7: Fixed bed performance at different length for a selected velocity (u= 2.574 cm/ min).

velocity in the bed was slower, increase the fluid residence time in the bed and the adsorbent has more opportunities to adsorb.

Effect of Fluid Velocity on the Bed Operation

The effect of various fluid velocities on a bed with a specific dimension was investigated. The fixed bed

Table 7: Specification of a typical fixed bed.

Variable	Unit	Value
Bed diameter	m	1.5
Bed length	m	4.5
Bed volume	m^3	7.95
Feed flow rate	cm^3/min	20202
Base velocity	cm/min	1.143
Selected velocities	cm/min	1.143- 2- 3
Initial sulfur conc.	ppm	5000

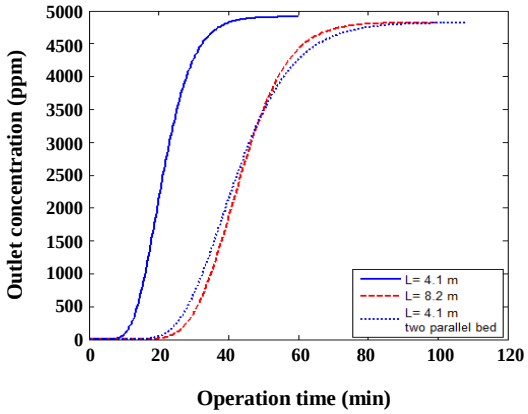

Fig. 8: Comparison of three methods to obtain the bed dimensions.

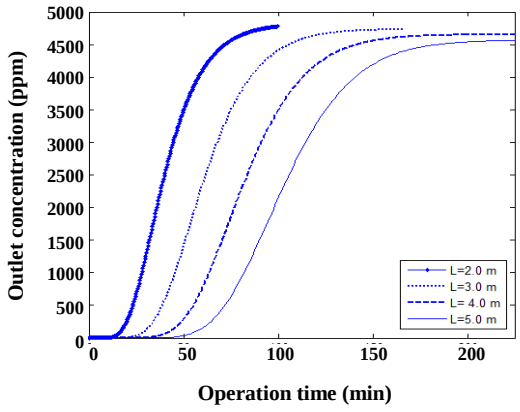

Fig. 9: Effect of fluid velocity on the bed operation.

the specification has been reported in Table 7. By passing the fluid through the bed with different velocities, the curves are shown in Fig. 9 are obtained.

As shown in Fig. 9 the bed performance has significantly affected by increase the fluid velocity or in the other word, feed flow rate, so that by increasing the velocities from 1.143 cm/min to 3 cm/min, the bed saturation time, i.e. reach to 500 ppm, decreases from 142 minutes to 52 minutes, which implies a lack of sufficient residence time for the fluid in bed.

Effect of the Bed Porosity

The effect of the bed porosity, void fraction, on the bed performance was investigated. Porosity reduction means reducing pore fluid passing through the bed, and this leads to increased velocity. We consider the bed with the specification that mentioned in Table 7 and the effect of changes in porosity observed. As shown in Fig. 10, the effect of decreasing the porosity such as by increasing the fluid velocity.

Effect of Initial Concentration of Thiophenic Compound

The initial concentration of sulfur in feed varies between 5000 ppm to 10000 ppm. With constant taking into account other parameters such as flow rate and porosity, for a typical dimension bed, the effect of the initial concentration of adsorbate on outlet concentration profile was investigated. It is observed from Fig. 11 that as the inlet sulfur concentration increases from 5000 ppm to 10000 ppm the break point time decreases without considering the velocity variation. For larger feed concentration, steeper breakthrough curves are found, because of the lower mass-transfer flux from the bulk solution to the particle surface due to the weaker driving force.

Pressure Drop during the Bed and Effective Variables

As mentioned before, the Ergun equation is appropriate for evaluating pressure drops in both laminar and turbulence regimes. Variables affecting the pressure drop are porosity, fluid velocity and particle diameter.

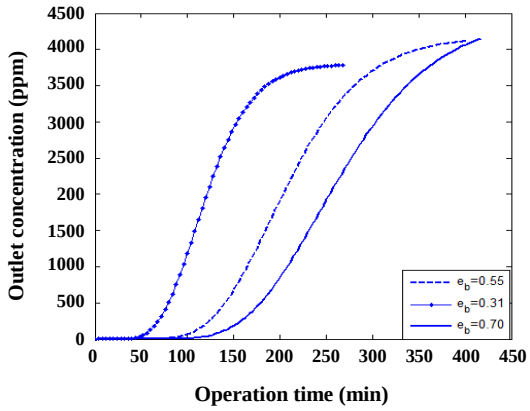

Fig. 10: Effect of the bed porosity.

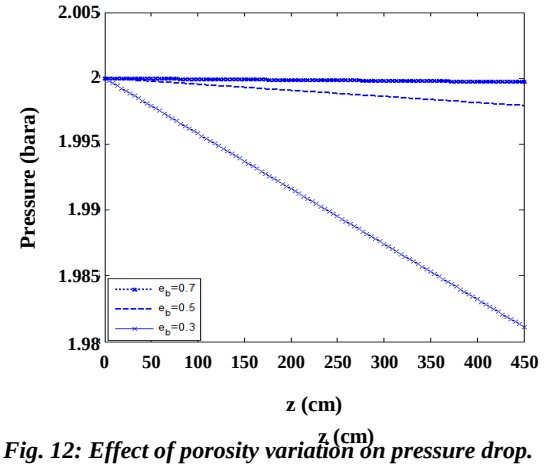

Fig. 12: Effect of porosity variation on pressure drop.

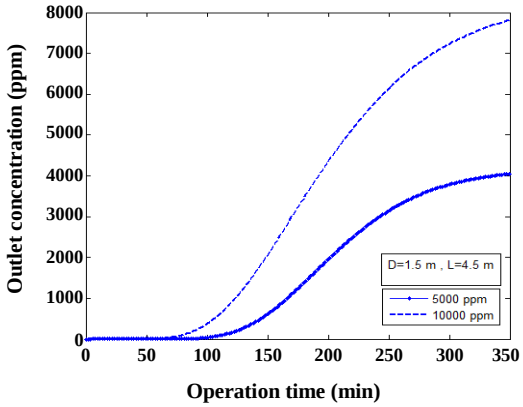

Fig. 11: Effect of the initial concentration of the thiophenic compound.

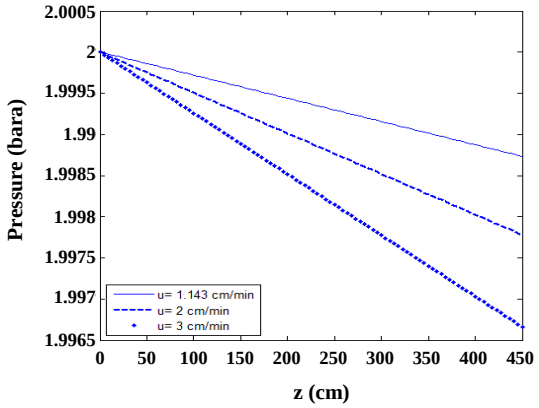

Fig. 13: Effect of velocity variation on pressure drop.

Effect of Porosity Variation on Pressure Drop

The effect of porosity variation on pressure drop is shown in Fig. 12. The pressure drop within the bed decreases by increasing the porosity. In fact, with an increase in porosity, the fluid velocity within the bed decreases and the velocity has a direct relation with pressure drop.

Effect of Velocity Variation on Pressure Drop

To investigate the effect of velocity variation we use a bed with specification reported in Table 7 and the results are shown in Fig. 13. By increasing the velocity from 1.143 cm/min to 3 cm/min, the pressure decreases from 1.999 bar to 1.997 bar, i.e. 2 mbar. Therefore, we can neglect the pressure drop at relatively low velocities as a reasonable assumption.

Effect of Particles Diameter on Pressure Drop

To investigate the effect of particles diameter we use a bed with specification reported in Table 7 and the results are shown in Fig. 14. Reduction in adsorbent diameter from 2cm to 0.5 cm leads to the pressure drop of 20 mbar which compared with two other factors, i.e. velocity and porosity, has a significant influence on pressure drop so that we cannot ignore its effect on pressure drop within the bed.

Mass Transfer Resistance

As mentioned before, the overall mass transfer coefficient, k_m, is caused by two mass transfer resistances which are consecutive. The first is mass transfer resistance in the fluid film around the adsorbent and the second is mass transfer resistance within the adsorbent pores. For a bed with specification reported in Table 7 the mass transfer coefficients are reported in Table 8. Since the mass transfer coefficient in adsorbent pores is much smaller than the film mass transfer coefficient, so the majority of mass transfer resistance is caused by diffusion into the adsorbent pores.

Table 8: Mass transfer coefficient calculated by software.

Parameter	Unit	Value
$k_{f,\ film}$	m/s	$3.556*10^{-5}$
$k_{s,\ adsorbent\ pores}$	m/s	$1.625*10^{-7}$

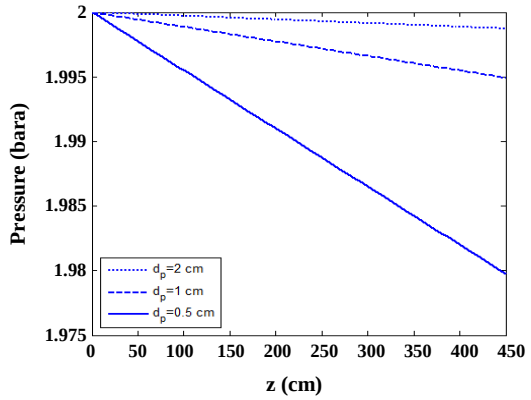

Fig. 14: Effect of particle diameter on pressure drop.

CONCLUSIONS

The isotherm model for DBT adsorption is described by both Langmuir and Freundlich equations and the results indicate that both Langmuir and Freundlich isotherms well predict the behavior of this adsorption process. In this work, the Langmuir model was employed and the corresponding parameters were used in scale up calculations.

The first step in the scale up calculations is to determine fluid velocity. There are three ways to choose fluid velocity. According to Mc. Cabe, in scale up, superficial velocity is the same in both large scale and small scale. Another way is using maximum allowable fluid velocity provided by *Ruthven et al.*. The third method is to select a fluid velocity between the two above values. The bed performance has significantly affected by increasing the fluid velocity or in the other word, feed flow rate, so that by increasing the velocities from 1.143 cm/min to 3 cm/min, the bed saturation time, i.e. reach to 500 ppm, decreases from 142 minutes to 52 minutes, which implies a lack of sufficient residence time for the fluid in bed. Among the parameters affecting the stability of an adsorption bed, observed that the fluid velocity is a key parameter in designing a bed, both laboratory scale and industrial scale. Increase in the fluid velocity leads to the reduction in the residence time of the fluid in the bed and adsorbent bed is saturated faster. Also in case of constant feed flow rate, an increase in fluid velocity, will decrease the cross sectional area of the bed and consequently the bed diameter. The second most affecting factor on bed stability is the initial concentration of contaminants in the feed. In addition, increasing the fluid velocity leads to more pressure drop, but not too much. So we can say that in low fluid velocity ranges, it is possible to neglect the pressure drop.

The most affecting factor on pressure drop through the bed is adsorbent particle diameter. It is not possible to neglect this effect and in any design, it should be calculated to do not exceed the allowable limit. Reduction in adsorbent diameter from 2cm to 0.5 cm leads to pressure drop of 20 mbar which compared with two other factors, i.e. velocity and porosity, has a significant influence on pressure drop so that we cannot ignore its effect on pressure drop within the bed.

Also, the mass transfer coefficient in adsorbent pores is much smaller than the film mass transfer coefficient, so the majority of mass transfer resistance is caused by diffusion into the adsorbent pores.

Notation

A	Cross section area, m^2
a_p	Specific surface area, m^2/m^3
Bio	Biot number
C	Concentration of solute, ppm
C_0	Initial concentration in bulk, ppm
C_s	Concentration on the adsorbent surface, ppm
C_e	Equilibrium concentration of solute, kg/m^3
C_p	Concentration of solute in adsorbent pores, ppm
Cp_s	Heat capacity of adsorbent, kJ/kg.K
D	Diffusion coefficient, m^2/s
D_p	Effective pore diffusion coefficient, m^2/s
D_m	Pore diffusion coefficient, m^2/s
D_s	Surface diffusion coefficient, m^2/s
D^*_s	Effective surface diffusion coefficient, m^2/s
D_{az}	Axial dispersion coefficient, m^2/s
g_c	Gravitational acceleration, m/s^2
h	Convective heat transfer, W/K

H_{ads}	Heat of adsorption, kJ/mol
i	Solute symbol
J	Diffusion flux, kg/m^2.s
J_p	Pore diffusion flux, kg/m^2.s
J_s	Surface diffusion flux, kg/m^2.s
K_{az}	Axial Conductivity, W/m.K
K_L	Langmuir isotherm coefficient, m^3/kg
K	The number of place divisions over the bed
k_f	Film mass transfer coefficient, m/s
K_F	Freundlich isotherm coefficient, (mg/g)(kg/g)$^{1/n}$
$K_{overall}$	Overall mass transfer coefficient, m/s
L	Bed length, cm
M	Molecular weight, mol/g
N	The number of time divisions
N_i	Mass transfer flux, kg/m^2.s
n	Freundlich isotherm constant
P	Pressure, bar
ΔP	Pressure drop, bar
Pe	Peclet number
q	Amount of solute adsorbed per gram of adsorbent, mg/g Ads
q_m	Maximum adsorbent capacity, mg S/g ads
r_m	*Stokes*-Einstein *radius*, m
Re	Reynolds number
R_p	Adsorbent radius, cm
Sc	Schmidt number
Sh	Sherwood number
t	Time, s
T	Absolute temperature, K
u	Fluid velocity, m/s
x	Dimensionless concentration
y	Dimensionless concentration

Greek symbols

π	Pi number (3.1415)
ε_b	Bed porosity
ε_p	Particle porosity
μ	Dynamic viscosity, cP
Φ	Association parameter
υ	Kinematic viscosity, cSt
v_A	Molar volume, cm^3/gmol
γ	Axial dispersion term
ρ	Fluid density, kg/m^3
ρ_b	Bulk adsorbent density, kg/m^3
ρ_s	Adsorbent density, kg/m^3

Received : Jan. 19, 2018 ; Accepted :Jun. 18, 2018

REFERENCES

[1] Muzic M., Sertic-Bionda K., Gomzi Z., Podolski S., Telen S., Study of Diesel Fuel Desulfurization by Adsorption, *Chemical Engineering Research and Design*, **88**: 487-495 (2010).

[2] Alhamed Y.A., Bamufleh H.S., Sulfur Removal from Model Diesel Fuel Using Granular Activated Carbon from Dates' Stones Activated by $ZnCl_2$, *Fuel*, **88**(1): 87-94 (2009).

[3] Seredych M., Bandosz T.J., Adsorption of Dibenzothiophenes on Nanoporous Carbons: Identification of Specific Adsorption Sites Governing Capacity and Selectivity, *Energy & Fuels*, **24**(6): 3352-3360 (2010).

[4] Triantafyllidis K.S., Deliyanni E.A., Desulfurization of Diesel Fuels: Adsorption of 4, 6-DMDBT on Different Origin and Surface Chemistry Nanoporous Activated Carbons, *Chemical Engineering Journal*, **236**: 406-414 (2014).

[5] Bu J., Loh G., Gwie C.G., Dewiyanti S., Tasrif M., Borgna A., Desulfurization of Diesel Fuels by Selective Adsorption on Activated Carbons: Competitive Adsorption of Polycyclic Aromatic Sulfur Heterocycles and Polycyclic Aromatic Hydrocarbons, *Chemical Engineering Journal*, **166**: 207-217 (2011).

[6] Kim, Jae Hyung, et al. Ultra-Deep Desulfurization and Denitrogenation of Diesel Fuel by Selective Adsorption Over Three Different Adsorbents: A Study on Adsorptive Selectivity and Mechanism, *Catalysis Today*, **111**(1): 74-83 (2006).

[7] Baltzopoulou, Penelope, et al. Diesel Fuel Desulfurization via Adsorption with the Aid of Activated Carbon: Laboratory-and Pilot-Scale Studies, *Energy & Fuels*, **29**(9): 5640-5648 (2015).

[8] Wang Y.e, Yang R.T., Desulfurization of Liquid Fuels by Adsorption on Carbon-Based Sorbents and Ultrasound-Assisted Sorbent Regeneration, *Langmuir*, **23**(7): 3825-3831 (2007).

[9] Moosavi E.S., Dastgheib S.A., Karimzadeh R., Adsorption of Thiophenic Compounds from Model Diesel Fuel Using Copper and Nickel Impregnated Activated Carbons, *Energies*, **5**: 4233-4250 (2012).

[10] Nekoo S. H., Fatemi S., Experimental Study and Adsorption Modeling of COD Reduction by Activated Carbon for Wastewater Treatment of Oil Refinery, *Iranian Journal of Chemistry and Chemical Engineering (IJCCE)*, **32**: 81-89 (2013).

[11] Yusuff A., Popoola L., Omitola O., Adeodu A., Daniyan I., Mathematical Modeling of Fixed Bed Adsorption Column for Liquid Phase Solute: Effect of Operating Variables, *International Journal of Scientific & Engineering Research*, **4**: 811-822 (2013).

[12] Seredych M., Bandosz T.J., Selective Adsorption of Dibenzothiophenes on Activated Carbons with Ag, Co, and Ni Species Deposited on Their Surfaces, *Energy Fuels*, **23**: 3737–3744 (2009).

[13] Shams A., Dehkordi A.M., Goodarznia I., Desulfurization of Liquid-Phase Butane by Zeolite Molecular Sieve 13x in a Fixed Bed: Modeling, Simulation, and Comparison with Commercial-Scale Plant Data, *Energy & Fuels*, **22**: 570-575 (2007).

[14] Babu B., Gupta S., Modeling and Simulation of Fixed Bed Adsorption Column: Effect of Velocity Variation, *i-Manager's Journal on Future Engineering and Technology*, **1**: 60- (2005).

[15] BagreevA., et al. "Bituminous Coal-Based Activated Carbons Modified with Nitrogen as Adsorbents of Hydrogen Sulfide, *Carbon*, **42**(3): 469-476 (2004).

[16] Faghihian H., Vafadar M., Tavakoli T., Desulfurization of Gas Oil by Modified Clinoptilolite, *Iranian Journal of Chemistry and Chemical Engineering (IJCCE)*, **26**(2): 19-25 (2007).

[17] Bakhtiari G., Bazmi M., Abdouss M., Royaee S.J., Adsorption and Desorption of Sulfur Compounds by Improved Nano Adsorbent: Optimization Using Response Surface Methodology, *Iranian Journal of Chemistry and Chemical Engineering (IJCCE)*, **36**(4) 69-79 (2017).

[18] Zhou A., Xiaoliang Ma, Chunshan Song. Effects of Oxidative Modification of Carbon Surface on the Adsorption of Sulfur Compounds in Diesel Fuel, *Applied Catalysis B: Environmental*, **87**(3):190-199 (2009).

[19] Ahmadi Nasab N., Hassani Kumleh H., Kazemzad M., Ghavipanjeh F., Application of Spherical Mesoporous Silica MCM-41 for Adsorption of Dibenzothiophene (A Sulfur Containing Compound) from Model Oil, *Iranian Journal of Chemistry and Chemical Engineering (IJCCE)*, **33**(3): 37-42 (2014).

[20] Xu Z., Cai J.-g., Pan B.-c., Mathematically Modeling Fixed-Bed Adsorption in Aqueous Systems, *Journal of Zhejiang University SCIENCE A*, **14**: 155-176 (2013).

[21] Bautista L., Martinez M., Aracil J., Adsorption of α-Amylase in a Fixed Bed: Operating Efficiency and Kinetic Modeling, *AIChE Journal*, **49**: 2631-2641 (2003).

[22] Shaverdi G., Haghighat F., Ghaly W., Development and Systematic Validation of an Adsorption Filter Model, *Building and Environment*, **73**: 64-74 (2014).

[23] Nwabanne J.T., Igbokwe P.K., Kinetic Modeling of Heavy Metals Adsorption on Fixed Bed Column, *International Journal of Environmental Research*, **6**(4): 945-952 (2012).

[24] Abu-Lail L., Bergendahl J.A., Thompson R.W., Mathematical Modeling of Chloroform Adsorption onto Fixed-Bed Columns of Highly Siliceous Granular Zeolites, *Environmental Progress & Sustainable Energy*, **31**(4): 591-596 (2012).

[25] Crittenden J.C., Weber W.J., Predictive Model for Design of Fixed-Bed Adsorbers: Parameter Estimation and Model Development, *Journal of the Environmental Engineering Division*, **104**(2): 185-197 (1978).

[26] McCabe W.L., Smith J.C., Harriott P., "Unit Operations of Chemical Engineering", Vol. 5: McGraw-Hill, New York, (1993).

[27] Treybal R.E., "Mass-Transfer Operations", McGraw-Hill Book Company, New York (1980).

[28] Perry R.H., Green D.W., "Perry's Chemical Engineers' Handbook", McGraw-Hill Professional, (1999).

[29] Ruthven D.M., "Principles of Adsorption and Adsorption Processes", John Wiley & Sons, Inc. (1984).

[30] Ghorai S., Pant K.K., Investigations on the Column Performance of Fluoride Adsorption by Activated Alumina in a Fixed-Bed, *Chemical Engineering Journal*, **98**(1): 165-173 (2004).

[31] Kumagai S., Ishizawa H., Toida Y., Influence of Solvent Type on Dibenzothiphen Adsorption onto Activated Carbon Fiber and Granular Coconut-Shell Activated Carbon, *Fuel*, **89**(2): 365-371 (2010).

[32] Fallah R.N., Azizian S., Removal of Thiophenic Compounds from Liquid Fuel by Different Modified Activated Carbon Cloths, *Fuel Processing Technology*, **93**(1): 45-52 (2012).

[33] Legates D.R., McCabe Jr G.J., Evaluating the Use of Goodness of Fit Measures in Hydrologic and Hydroclimatic Model Validation, *J. Water Resour. Res.*, **35**: 233–241 (1999).